

# BUNDLE ADJUSTMENT OF IMAGES FROM NON-METRIC CCD CAMERA USING LIDAR DATA AS CONTROL POINTS

R. Delara Jr.<sup>a</sup>, E. A. Mitishita<sup>a</sup>, A. Habib<sup>b</sup>

<sup>a</sup> UFPR, Federal University of Parana, Department of Geomatics, Curitiba, Parana, Brazil, rls@ufpr.br, mitishit@ufpr.br

<sup>b</sup> UCalgary, Department of Geomatics Engineering, University of Calgary, Alberta, Canada – habib@geomatics.ucalgary.ca

## Commission III, WG I

**KEY WORDS:** Photogrammetry, LIDAR, DEM, Bundle, Non-metric, Digital, Camera.

### ABSTRACT:

The use of non-metric, low cost digital cameras is becoming a very attractive option as a source of spatial information about terrestrial surfaces. This is being motivated by the increased resolution of CCD sensors, as well as the results of recent studies indicating the stability of the internal parameters of such cameras. On the other hand, Digital Elevation Model obtained by laser scanning is an excellent source of reliable three-dimensional coordinates for several applications in photogrammetry and other fields. Although the Laser Scanner provides high reliable geometric information, it can not be compared to information contained in a digital image, because the spectral information of the laser system is very poor. Therefore, the integration of both data sources is an attractive option for mapping. The exterior orientation parameters crucial information to guarantee the quality of the resulting map from photogrammetric processing. These parameters could be computed in real time using an onboard GPS/INS unit or post processed using a LIDAR system together with a digital camera with bundle adjustment method. In this paper, is presented a methodology to perform the bundle block adjustment using non-conventional aerial images and Laser Scanner data. The images were taken with a Sony DSC-F717 digital camera, with a resolution of 5.2 Mb, CCD dimension of 2520 x 1960 pixels, covering about 2 km<sup>2</sup> of the Campus of the Federal University of Parana - Brazil. The elevation above ground of the aerial survey was about 750 meters and the pixel ground sample distance is about twenty five centimeters. The elevation above ground of the LIDAR survey was about 1000 meters. The LIDAR system used was an OPTECH ALTM 2050, which belongs to the Institute of Technology for Development LACTEC/UFPR. This system is characterized by a planimetric accuracy of fifty centimeters and altimetric accuracy of fifteen centimeters. Some check points were surveyed with conventional GPS techniques allowing for the comparison and evaluation of the precision/accuracy of the final results.

## 1. INTRODUCTION

New technologies, especially those proceeding from computer and electronic areas, have enabled the development of digital photogrammetry. Photogrammetric tasks, formerly dependent on sophisticated equipments and highly specialized technicians, are now being gradually substituted for autonomous photogrammetric procedures performed in a computer. Likewise, Global Positioning System (GPS) has simplified field operations necessary to survey ground control points while conducting photogrammetric tasks. For about fifteen years, Laser Scanning systems have improved and are being used to obtain altimetric information of the terrestrial surface. The accuracy levels reached are currently around one decimeter for altimetry and the double of this value for planimetry (Wever and Linderberger 1999). A Laser Scanner system is basically constituted of GPS, Inertial Navigation System (INS) and the LASER scanning device (Laser Rangefinder). The Laser Scanner system enables the determination of the spatial position of the points which reflect the laser ray emitted, thus generating a group of points irregularly distributed that can constitute the base of a Digital Elevation Model (DEM). The increasing availability of data generated by laser profiling, enabling higher accuracy in definition of relief representation and physical objects elevation on the surface, has improved photogrammetric procedures. On the other hand, digital cameras, with better spatial resolutions and low cost, have facilitated the acquisition

of digital images for photogrammetric application purposes. The integration of positional data proceeding from Laser Scanner with aerial digital images of a same region allows the development of new photogrammetric procedures. This paper presents the integration of LIDAR data with digital images obtained from an aerial covering utilizing a small-format digital camera, model SONY DSC-F717, which has a CCD sensor with resolution of 2560 x 1920 pixels (details Sony 2002). It presents the methodology developed and the results obtained, while conducting the triangulation by bundle method, of a block of digital images. The ground control points are originated in a scanning carried out with Laser Scanner. The pixel was utilized as the unit of measurement for photogrammetric observations and the determination of interior orientation parameters. This process was previously conducted using a technique of camera calibration (See Delara, 2003).

## 2. TEST AREA

In this research was used a block of digital images containing thirteen images distributed in two strips as presented in Figure 3. The region covered is part of the Campus of the Federal University of Parana. This region was surveyed by Laser Scanner with density of approximately 2.5 points by square meter. The Laser Scanner data were obtained on 05/09/2003 using the OPTECH ALTM 2050 system, property of the

Institute of Technology for Development – LACTEC / UFPR. The aerial survey was conducted on 06/27/2003, in a flying height of approximately 750 meters, resulting in a spatial resolution on the terrain of 0.25 meters.

### 3. BACKGROUND

Non-metric digital cameras are not provided with fiducial marks, which allow the recovery of the projective geometry. Having the need of a reference system to recover the geometry through a procedure of camera calibration, an intermediary referential, called image referential for the referencing of photogrammetric observations conducted on the image, was utilized in this research. The referentials of image space and object space employed in this work are:

#### 3.1 Reference System in the Image Space

- Digital System  $(x'', y'')$  defined as a two-dimensional rectangular system, left-handed system, with the origin at the image's left top corner, being  $x''$  coincident with the first line and  $y''$  coincident with the first column;
- Image System  $(x, y)$  is two-dimensional rectangular system coordinates with the origin in image's geometric center, right-handed system.

The two systems are assumed as being parallel. The transformation between digital and image systems can be done using the following equations (Jain et al. 1995):

$$x = x'' - \frac{Col + 1}{2} \quad (1)$$

$$y = \frac{Row + 1}{2} - y'' \quad (2)$$

$x'', y''$  = coordinates in the digital system;  
 $x, y$  = coordinates in the image system;

$Col$  = image's number of columns;  
 $Row$  = image's number of rows;

- the system of photogrammetric coordinates  $(x', y', c)$ , the photo coordinate system is a three-dimensional, rectangular, right-handed system with its origin at the perspective center and by definition parallel to image's referential (Merchant 1988). Knowing the coordinates of the principal point in the image's referential  $(x_0, y_0)$ , the transformation from one system into another takes place through a simple translation in the plan, as presented in equations 3 and 4.

$$x' = x - x_0 \quad (3)$$

$$y' = y - y_0 \quad (4)$$

$x', y'$  = photogrammetric coordinates;  
 $x_0, y_0$  = principal point coordinates (image system).

#### 3.2 Reference System in Space Object

The reference system for the space object, adopted for the present work, consists of a hybrid system in which the geodetic coordinates in the UTM projection system and SAD69 reference system (E,N) and the orthometric height (h), were equaled to the rectangular coordinates, respectively, X,Y,Z. The small area of approximately 2 km<sup>2</sup>, covered by the images, enabled the utilization of this hybrid coordinate referential without damage to the accuracy.

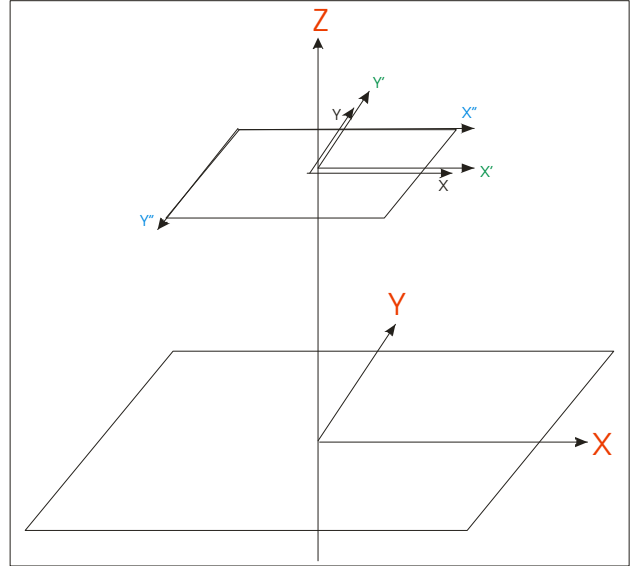


Figure 1. Reference Systems.

#### 2.3 Bundle Method

The block triangulation through bundle of convergent rays (bundle method) considers photogrammetric observations as a bundle of straight lines. Each straight line is defined by the condition of collinearity of three points (both image and object spaces points, and perspective center). The triangulation through bundle adjustment (BA) uses collinearity equations as fundamental mathematical model. These equations must be linearized to perform the adjustment using Least Squares Adjustment – LSA. Which is employed to determine the parameters of exterior orientation of the images involved and the coordinates of photogrammetric points observed (Lugnani, 1988). It can be considered to be the most precise and flexible triangulation method (Mikkail, Bethel, McGlone 2001). In this paper, the photogrammetric observations were previously corrected from systematic errors of the image, as presented in equations 6 and 7. The aerotriangulation program developed in MATLAB (BundleH) employed Combined adjustment method (Gemael 1994) with constraints of weight or position in the control points. Here follows the basic formulation:

$$F(La, Xa) = 0 \quad (5)$$

$La$  = vector of the observed values adjusted;  
 $Xa$  = vector of the adjusted parameters.

The components of systematic errors in the coordinates are calculated in the photogrammetric referential.

$$x' = x - x_0 - \delta r_x - \delta l_x - \delta a_x - \delta f_x \quad (6)$$

$$y' = y - y_0 - \delta r_y - \delta d_y - \delta a_y - \delta f_y \quad (7)$$

$$x' = -c \frac{m_{11}(X - X_0) + m_{12}(Y - Y_0) + m_{13}(Z - Z_0)}{m_{31}(X - X_0) + m_{32}(Y - Y_0) + m_{33}(Z - Z_0)} \quad (8)$$

$$y' = -c \frac{m_{21}(X - X_0) + m_{22}(Y - Y_0) + m_{23}(Z - Z_0)}{m_{31}(X - X_0) + m_{32}(Y - Y_0) + m_{33}(Z - Z_0)} \quad (9)$$

$$M = R_z(\kappa) \cdot R_y(\varphi) \cdot R_x(\omega) \quad (10)$$

$$M = \begin{bmatrix} m_{11} & m_{12} & m_{13} \\ m_{21} & m_{22} & m_{23} \\ m_{31} & m_{32} & m_{33} \end{bmatrix} \quad (11)$$

$$m_{11} = \cos \varphi \cdot \cos \kappa$$

$$m_{12} = \cos \omega \cdot \sin \kappa + \sin \omega \cdot \sin \varphi \cdot \cos \kappa$$

$$m_{13} = \sin \omega \cdot \sin \kappa - \cos \omega \cdot \sin \varphi \cdot \cos \kappa$$

$$m_{21} = -\cos \varphi \cdot \sin \kappa$$

$$m_{22} = \cos \omega \cdot \cos \kappa - \sin \omega \cdot \sin \varphi \cdot \sin \kappa$$

$$m_{23} = \sin \omega \cdot \cos \kappa + \cos \omega \cdot \sin \varphi \cdot \sin \kappa$$

$$m_{31} = \sin \varphi$$

$$m_{32} = -\sin \omega \cdot \cos \varphi$$

$$m_{33} = \cos \omega \cdot \cos \varphi$$

$c$  = camera constant;

$X, Y, Z$  = ground coordinates;

$X_0, Y_0, Z_0$  = ground coordinates of the perspective centre;

$m_{ij}$  = elements of the rotation matrix  $M$ ;

$\delta r_x$  e  $\delta r_y$  = symmetric radial distortion correction;

$\delta d_x$  e  $\delta d_y$  = decentering distortion correction;

$\delta a_x$  e  $\delta a_y$  = affine deformation correction;

$\delta f_x$  e  $\delta f_y$  = photogrammetric refraction correction.

### 3.4 LIDAR

The laser profiling system generates a cloud of points irregularly distributed on the terrestrial surface. Its three-dimensional coordinates in a geodetic system are determined in function of the time of emission and return of a laser pulse. This process is called *Light Detection and Ranging* – LIDAR (Optech, 2003). A precise laser rangefinder scans the surface registering the pulses (distances). To correct the movements of the aircraft during the post-processing, the Euler angles ( $\kappa, \varphi, \omega$ ) referring to each distance measured are determined through INS, during profiling. The positioning of the aircraft is determined by GPS through two receptors, one installed in the aircraft and other on the terrain, thus enabling differential correction and refinement of the coordinates (Figure 2). During the post-processing, the data generated are combined and determine the precise position of the ground points. The nominal precision of the system is around 15 cm (mean square error) for altimetry and around 30 cm for planimetry (Wever and Linderberg 1999, Optech 2003). See more details in Baltsavias, 1999.

## 4. METHODOLOGY

This research was carried out in two basic stages. The first stage verified the positional quality of the Laser Scanner data and the second one implemented procedures to carry out the triangulation through simultaneous adjustment of images (Bundle method), supported by data coming from the Laser Scanner.

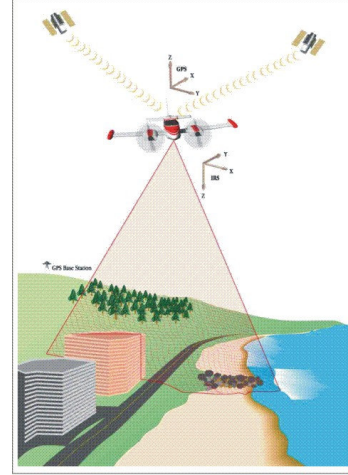


Figure 2. LIDAR (Optech 2003).

### 4.1 Verification of LIDAR Positional Quality Data

To verify the positional quality of the Laser Scanner data existing in the work area, as reference, it was utilized 8 points, positioned by geodetic techniques (GPS and geometric leveling), which have planialtimetric coordinates with accuracy of few millimeters. These verification points are identifiable details in the intensity image generated with data from the Laser Scanner. On the terrain, they are concrete marks in the form of a pyramidal trunk with dimensions of 20 x 40 cm and approximate height of 30 cm in relation to the soil, and are distributed all over the test area (they are identified with \* in Figure 4). The intensity image employed in this research was obtained from a regular grid with spacing of 40 cm. The intensity image was employed just to obtain the approximate coordinates of the points of verification selected. These approximate coordinates are input data in the search for the non-interpolated coordinates in the original text file proceeding from the Laser Scanner. The search process entailed the following stages:

- in the original file, the neighbor points are separated to the approximate coordinate within a 1 m radius circle.

- for the definition of the point coordinate, two criteria must be met: firstly, the proximity, and the secondly, the point researched must be the point of highest altitude (h).

From the comparison of the geodetic coordinates of the check points and the respective generated by LIDAR, one has the results presented in Table 1.

The average planimetric discrepancy (dR) obtained in the verification conducted between the coordinates of the verification points and the ones obtained from LIDAR was of 0.254 m. The averages resulting in dN, dE show a normal distribution of the discrepancies obtained, exempting the data from possible systematic errors. The results obtained in the

altimetry also show a normal distribution in the residues and a standard error of 0.109 m. The accuracy results obtained in this verification are compatible with the nominal precision offered by the manufacturer of the system.

Point	dN(m)	dE(m)	dR(m)	dh(m)
RN02	-0.020	0.215	0.216	0.085
RN03	-0.215	-0.019	0.216	0.053
RN08	-0.006	0.136	0.136	-0.050
RN09	-0.001	0.121	0.121	-0.009
RN12	0.321	-0.120	0.343	-0.168
RN14	-0.227	0.315	0.388	-0.133
RN21	-0.032	-0.397	0.398	0.013
RN23	-0.169	-0.130	0.213	0.192
mean	-0.044	0.015	0.254	-0.002
s.d.	0.164	0.214	0.102	0.109

Table 1. LIDAR verification

#### 4.2 Triangulation

Firstly, utilizing intensity image (Figure 5.a) and aerial image (Figure 5.b), thirty-five details that were identifiable in both images and that were in the necessary geometric position to carry out triangulation were selected, as shown in Figure 4. To meet the search criteria in the original Laser Scanner data, these points were always defined on the top of the objects selected. Utilizing the program ENVI 3.4 and the intensity image, the planimetric coordinates (approximate) of the points selected were extracted;

- employing the same procedure used in item 4.1, the planimetric coordinates of thirty five points selected were determined in the original text file proceeding from the Laser Scanner;

- exemplifying the procedure for Point 8, of approximate coordinates E = 677677.76 m and N = 7184398.63 m, one has in Table 2 the selected points in a 1 m ray circle.

Point	E(m)	N(m)	h(m)	d(m)
8.1	677677.540	7184398.420	924.310	0.304
8.2	677678.230	7184398.830	923.660	0.511
8.3	677677.210	7184399.140	914.750	0.750
8.4	677678.520	7184398.320	923.560	0.821
8.5	677677.690	7184397.800	924.470	0.833
8.6	677677.660	7184399.600	919.830	0.975

Table 2. Original coordinates researched for the Point 8.

Table 2 shows that point 8.1 meets the criteria of proximity and highest altitude.

Out of the group of thirty-five points, nine points of planimetric control in the periphery of the block were selected, twenty-one of altimetric control and five of verification. Employing the program ENVI 3.4, the manual reading of the photogrammetric points selected in the thirteen images taking part of the block to be triangulated was performed. The coordinates were obtained in the digital system and next transformed into the

photogrammetric system with proper corrections of systematic errors. Finally, the processing of triangulation with the program BundleH was conducted. As far as the ground control points existing in the triangulated block are concerned, it was decided that the control points planialtimetrically constrained occupied the periphery of the block, so as to be minimum in number and to leave the biggest area possible in the interior of this block occupied by point with altimetric constraint.

The final distribution of the triangulated points and of verification (without any constraint), may be observed in Figure 4.



Figure 3. Block of Digital Images from Sony DSC-F717.

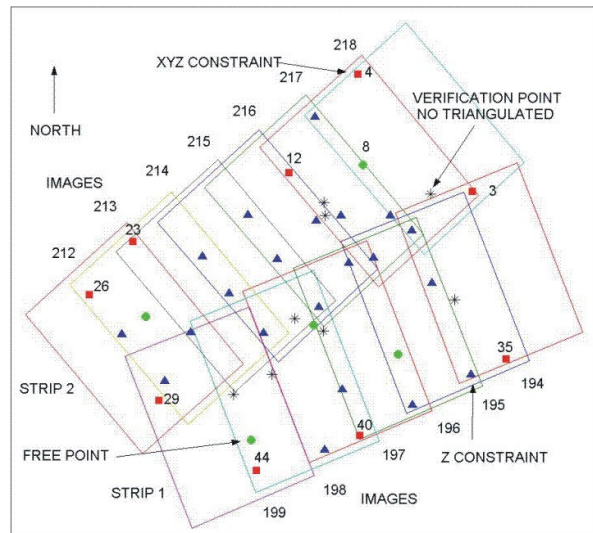


Figure 4. Triangulated Block.

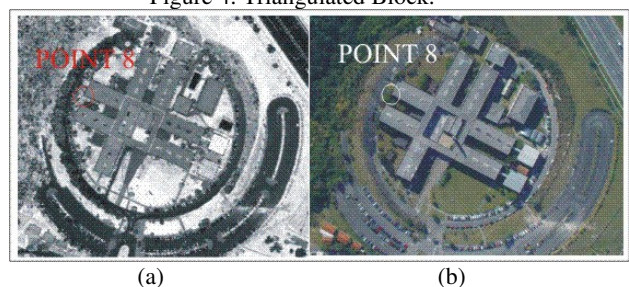


Figure 5. Intensity image (a) and digital image (b).

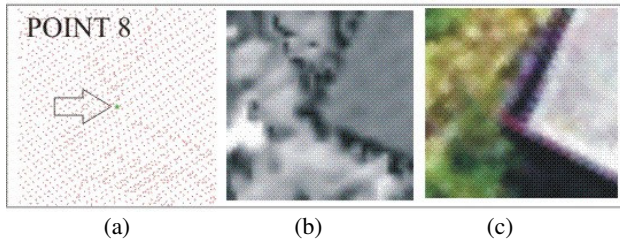


Figure 6 – (a) LIDAR cloud of points (the Point 8 is in the central area); (b) detail for the Point 8 in the intensity image; (c) detail of the Point 8 in the photographic image.

## 5. RESULTS

The results obtained in the processing of triangulation are within the precision levels appropriate for photogrammetric observations and for coordinates of ground control points. Firstly, a global analysis of the adjustment carried out was considered utilizing the statistical test of the qui-square, based on the *a priori* (1.0) and *a posteriori* (0.196674) variance. It was verified that the residues obtained in the observations conducted are all below a pixel, what corresponds to 25 cm on the terrain. Comparing the planimetric coordinates of the altimetric constrained control points obtained from the triangulation and the ones proceeding from the laser scanning, it is verified in Table 3 an average planimetric result of 0.513 meters, with standard deviation of 0.258. This shows that 68.8% of the points tested are within a planimetric accuracy below 80 cm and 100% of the points tested below 1.0 meter. Table 4 displays the results obtained in the points of verification. In this case, the planimetric discrepancies obtained are smaller, but not significant considering the small number of points analyzed and standard deviation obtained. Therefore, the conclusion is that the planimetric accuracy obtained in the experiment conducted is around 75 cm and the altimetric around 80 cm.

## 6. CONCLUSIONS AND RECOMMENDATIONS

The results obtained in this research were encouraging and led to the following conclusions:

- the methodology employed for the utilization of LIDAR data and determination of points of altimetric and planimetric control for triangulation was considered efficient;
- low-cost digital cameras may be employed in low-cost aerophotogrammetric surveys;
- the utilization of non-simultaneous aerial surveys with LIDAR is promising for future applications in cartographic updating;
- the utilization of the *pixel* as a unit in the image system was consistent and efficient;
- the integration of LIDAR data with aerial images obtained with small-format digital cameras was perceived as promising considering the progressive resolution increase in the area sensors of these cameras and the increasing number of regions surveyed with LIDAR.

Point	dE(m)	dN(m)	dR(m)	dh(m)
7	0.214	-0.181	0.280	0.016
11	0.252	-0.204	0.324	-0.015
13	0.201	-0.339	0.394	-0.005
14	-0.354	-0.278	0.450	-0.094
15	-0.236	-0.120	0.265	0.018
16	0.484	-0.726	0.873	0.014
17	0.251	0.489	0.550	0.014
18	0.208	0.062	0.217	-0.015
19	0.004	-0.157	0.157	0.047
20	-0.293	0.595	0.663	-0.005
21	0.313	-0.438	0.538	-0.025
22	0.093	0.284	0.299	-0.042
24	-0.185	-0.104	0.212	0.030
27	-0.097	0.879	0.884	0.030
28	0.650	0.189	0.677	0.000
32	-0.141	0.293	0.325	0.087
33	-0.551	0.416	0.690	-0.030
34	0.259	-0.883	0.920	0.012
38	-0.836	0.178	0.855	0.001
39	-0.176	0.835	0.853	0.051
42	-0.331	0.092	0.344	0.001
mean	-0.013	0.042	0.513	0.004
s.d.	0.358	0.462	0.258	0.037

Table 3. Points with Altimetric Constraint.

Point	dE(m)	dN(m)	dR(m)	dh(m)
8	0.299	0.040	0.302	0.536
37	0.172	-0.123	0.211	-0.416
43	-0.585	0.219	0.625	0.736
90	-0.306	-0.588	0.663	-0.872
91	-0.136	-0.052	0.146	-0.436
mean	-0.111	-0.101	0.389	-0.090
s.d.	0.358	0.301	0.239	0.691

Table 4. Check Points (Free Points).

## References

- ANDRADE, R.R., 2001. Dedrometric Measures with Calibrated Digital Cameras. MSc. Dissertation. Portuguese. Curitiba, UFPR, 138p.
- BALTSAVIAS, E.P., 1999. Airborne laser scanning: basic relations and formulas. ISPRS Journal of Photogrammetry & Remote Sensing 54 (1999) 199-214p.
- DELARA, R., 2003. Calibration of Non Metric, Small format Digital Cameras Using the Pixel as unit in the Image Space. Portuguese. Curitiba, UFPR, 46p.
- GEMAEL, C., 1994. Introduction to Adjustment of Observations: Geodetic Applications. Portuguese. Curitiba: Ed. UFPR, 319p.

JAIN, R.; KASTURI, R.; SCHUNCK B.G.,1995. Machine Vision. McGraw-Hill, Inc. Singapore. 549p.

LUGNANI, J.B., 1988. Introduction to Phototriangulation. Curitiba: ed UFPR, 134p.

MERCHANT, D.C., 1988. Analytical Photogrammetry: Theory and Practice. Part I, Columbus, Ohio, Department of Geodetic Science, The Ohio state University.

MIKHAIL, E.M.; BETHEL, J.; McGLONE, J.C., 2001. Introduction to Modern Photogrammetry. 479p.

SONY, 2002. Digital Still Camera Cybershot DSC-F717. Sony Corporation, 121p.

WEVER C., LINDEBERGER J., 1999. Experiences of 10 years laser scanning. [www.ifp.uni-stuttgart.de/publications/phowo99/wever.pdf](http://www.ifp.uni-stuttgart.de/publications/phowo99/wever.pdf), 125-132p.

<http://www.optech.on.ca> (accessed 5/25/2003)

Processing

Iteration = 15

Convergency = 0.000001

SigmaPosteriori = 0.196674

Global Test – significance 5%

OK if  $Q2_{table} \geq Q2_{computed}$

$Q2_{computed}$  19.08

$Q2_{table}$  30.24

Passed.

Image Observations Residues

V(Rxy) 0.362 (pixel) Mean

V(Rxy) 0.204 (pixel) Standard Deviation

V(Rxy) 0.919 (pixel) Max Resultant

V(Rxy) 0.040 (pixel) Min Resultant

## Appendix – Triangulation data

Program: BundleH

Site: Centro Politecnico - UFPR - Curitiba - Parana - Brazil.

Camera : Sony DSC-F717 - resolution 2560 x 1920 pixel

Calibration information: ( unit = pixel )

Focal Length : 2931.722

Coordinate x of Principal Point : -71.648

Coordinate y of Principal Point : -40.965

Symmetric Radial Distortion Coefficients:

K1 = -2.63950e-008

K2 = 3.24240e-015

K3 = 3.06100e-022

Decentric Distortion Coefficients:

P1 = -4.13010e-007

P2 = 2.42890e-007

Affine Deformation Parameters:

A = -1.34550e-004

B = -2.03270e-005

Photogrammetric Refraction

Atmospheric Refraction e45 Coefficient : 9.32533e-006

(Saastamoinen Model)

Flight information :

Average terrain height above sea level : 909.394 m

Average flying height above sea level : 1648.583 m

Average flying height above terrain : 739.189 m

Number of Images : 13

Pixel Ground Sample Distance : 0.252 m

Adjustment input:

Ground Points Observations Standard Deviation : 0.250 m

Image Observations Standard Deviation : 1.0 pixel

Sigma Apriori (*a priori* variance of unit weight): 1.0

Number of Parameters (EO) = 6 x n° of images : 78

Coordinates = 3 x n° of points : 105

Observation Equations = 2 x n° of observations : 190

Number of Constraints Equations : 90

Redundancy : 97